



A₂B corrole with a *meso*-[Pt^{II}(bipy)Cl₂]-substituent: Synthesis, electronic structure and highly efficient electrocatalyzed hydrogen evolutions

Yingxin Guo^{a,1}, Tingting Gu^{b,1}, Pengfei Li^a, Bo Fu^{a,d}, Lei Sun^{a,d}, Weihua Zhu^{b,c}, Haijun Xu^{a,d,*}, Xu Liang^{b,c,*}

^a Jiangsu Co-Innovation Center of Efficient Processing and Utilization of Forest Resources, College of Chemical Engineering, Nanjing Forestry University, Nanjing 210037, PR China

^b School of Chemistry and Chemical Engineering, Jiangsu University, Zhenjiang 212013, PR China

^c State Key Laboratory of Coordination Chemistry, Nanjing University, Nanjing 210000, PR China

^d Jiangsu Key Lab of Biomass-based Green Fuels and Chemicals, Nanjing Forestry University, Nanjing 210037, PR China



ARTICLE INFO

Keywords:

Platinum corrole
Electronic structure
Hydrogen evolution
Spectroscopy
Electrochemistry

ABSTRACT

Synthesis and electronic structure of *meso*-2,2'-bipyridine substituted H₃corrole and its Pt(II) complex were described. This study demonstrates that A₂B type corrole containing *meso*-[Pt^{II}(bipy)Cl₂] substituents are highly efficient catalysts for hydrogen evolutions with low overpotential (50 mV vs RHE), low Tafel slope (59 mV/dec) and robust catalytic behaviors. The efficient catalytic properties can be readily enhanced by charge transfer between bridging conjugated aromatic ring (corrole) and *meso*-[Pt^{II}(bipy)Cl₂] catalytic center.

1. Introduction

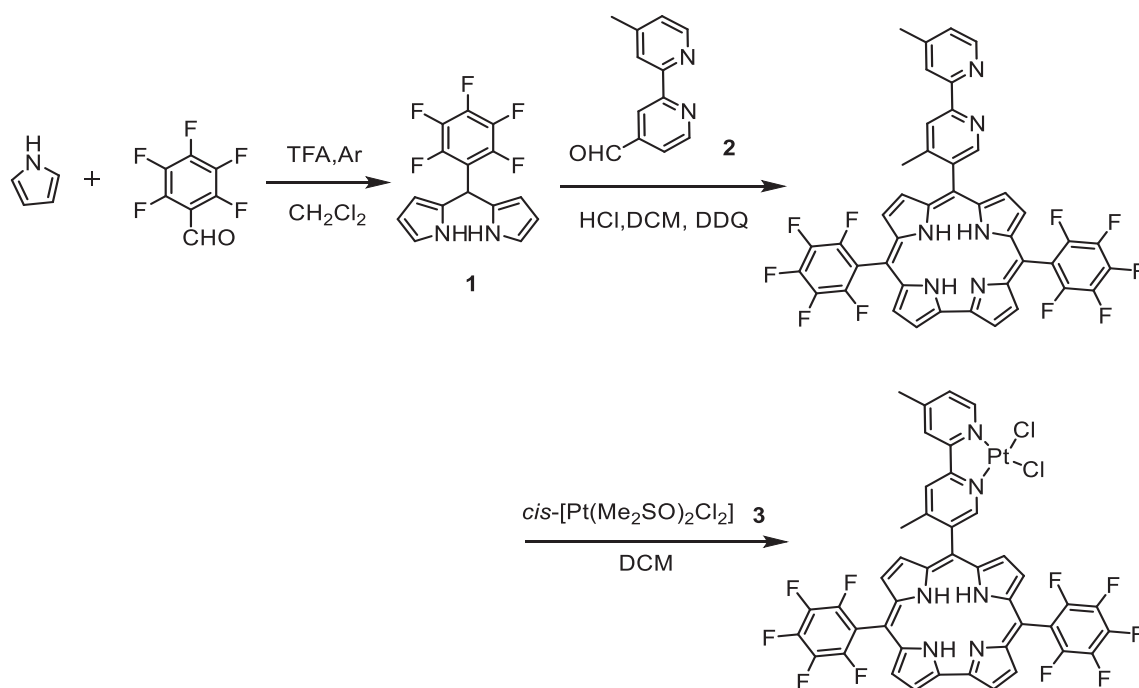
The frontier research of hydrogen for energy storage so that supply from renewable sources can be balanced with demand through the use of fuel cells has many advantages to rationally replace the use of fossil fuels in many contexts [1–3]. Within in this aim, there has been increased interests in hydrogen evolution reactions (HERs) that involve the reduction of protons, due to the straight forward procedures that are involved and the availability of catalytic materials to convert electrical energy to chemical energy through the generation of H₂ gas [4–6]. In addition to investigate the tunable catalytic behaviors through chemical catalysis, photocatalysis and electrocatalysis [7–9], to rational design and prepare of highly efficient catalysts are the key points [10–12]. On the other hand, recent researches have indicated that molecular electrochemical catalysis exhibit various advantages, including highly efficient, tunable and stable catalytic behaviors that afforded further perspectives [13,14]. Corroles, porphyrin analogues with a direct pyrrole-pyrrole bond and an extra NH proton on the inner ligand perimeter, have applied as functional catalysts in several different types of reactions including organic synthesis, the removal of environmental harmful pollutants [15], and efficient energy conversions (such as HERs) [1,16–18]. Moreover, platinum coordinated

complexes and composites have revealed outstanding catalytic behaviors including low overpotential, low Tafel slope and stable for large number of cycles [19–21], but the platinum contained metallocorroles have never been described before in the same system. This is because of the lack of research of platinum corrole. Till now as our best knowledge, platinum(IV) corroles, of which there has been only few reports accessible via a low yielding, but are particularly intriguing because of their potential for axial reactivity [22,23]. In addition, to introduce 2nd ligand at the *meso*-positions are also the effective strategies to stabilize platinum atom at the corrole system at novel that could be applied in a wide range of applications, such as biochemistry [24]. On the other hand, platinum coordinated complexes also have several advantages in the field molecular engineering and their applications in various catalytic fields [25–27]. In this paper, 2,2'-bipyridine was used as a functional *meso*-substitutes to facilitate synthesis and characterize *meso*-[Pt^{II}(bipy)Cl₂]-substituted H₃corrole that corrole will play the effective electron transfer media to construct the rGO supported Pt(II)corrole system for stably and electrochemically catalyzed hydrogen evolutions, and the electronic structure investigations will also be described.

* Corresponding authors at: Jiangsu Co-Innovation Center of Efficient Processing and Utilization of Forest Resources, College of Chemical Engineering, Nanjing Forestry University, Nanjing 210037, PR China (H. Xu). School of Chemistry and Chemical Engineering, Jiangsu University, Zhenjiang 212013, PR China (X. Liang).

E-mail addresses: xuhaijun@njfu.edu.cn (H. Xu), liangxu@ujss.edu.cn (X. Liang).

¹ These authors were contributed equally.



Scheme 1. A₂B Corrole with a *meso*-bipyridine **4** and *meso*-[Pt^{II}(bipy)Cl₂]-substituent **5**.

2. Experimental section

2.1. General

¹H NMR spectra were recorded on a Bruker AVANCEIII 600 M spectrometer. UV–Vis spectra were recorded on Shimadzu UV-2600 spectrophotometer at ambient temperature with a 1 cm quartz cell. ESI-MS was performed in a Bruker Daltonik, GmbH (Bremen), mass spectrometer equipped with an electrospray ionization (ESI) source. Cyclic voltammetry was performed with a three-electrode-compartment cell in *o*-dichlorobenzene (*o*-DCB) solutions with 0.1 M [n-Bu₄N](ClO₄) as supporting electrolyte using CHI-730D electrochemistry workstation. A glassy carbon electrode of diameter 3 mm was used as the working electrode while platinum wire and Ag/AgCl electrodes were used as the counter and reference electrodes respectively.

2.2. Preparation of modified electrodes

1.0 mg rGO was mixed with 1 mL isopropyl alcohol containing 0.2% nafion and the mixture sonicated in ultrasonic bath for 30 min to produce a homogeneous mixture of concentration 1 mg/mL. The surface of the glassy carbon electrode (GCE) was polished with 0.05 μm alumina and rinsed with doubly distilled water in ultrasonic bath to remove any adhered Al₂O₃ particles. The electrodes were rinsed with ethanol and dried under room temperature for about 5 min. Three times 3 μL of the rGO/isopropyl alcohol/nafion suspension was drop casted on the surface of the GC electrode and allowed to dry at room temperature. A 10 μL of 0.2 mM THF solutions of **5** was added dropwise to three different rGO/nafion-coated electrodes and dried at room temperature for 1 h.

2.3. Synthesis of **2**

4,4-dimethyl-2,2'-bipyridine (10 mmol, 1.8 mg), SeO₂ (12 mmol, 1.3 mg) and water (3 mL) were dissolved in 20 mL dioxane and stirred at 90 °C for 24 h under Ar. After cooling to the room temperature, 0.3 M sodium pyrosulfite (Na₂S₂O₅) solution (50 mL) was added and stirred again at room temperature. Then, the pH value was adjusted by

NaHCO₃ to neutralized value and the mixture was extracted by CH₂Cl₂ (50 mL×3). The target compound was finally obtained after distillation to give the white solid compound in a 44% yield (870.2 mg). ¹H NMR (CDCl₃, 600 MHz, ppm) δ 10.21 (1H), 8.92 (d, *J* = 12 Hz, 2H), 8.61 (s, 1H), 8.31 (s, 1H), 8.74 (s, 1H), 2.49 (s, 3H).

2.4. Synthesis of **3**

Potassium hexachloroplatinate (1.0 g) was slowly dissolved in 10 mL and DMSO (0.6 mL) was added. The light-yellow crystals were slowly observed over 3 h, and all solid compounds were collected. After washing by water, ethanol and ether, the target compound *cis*-[Pt(Me₂SO)₂Cl₂] **3** was finally obtained in an 89% yield (89.7 mg).

2.5. Synthesis of **4**

The general synthetic procedure was followed literature reported procedure whereas arylaldehyde **2** was used instead, and the target compound was successfully isolated from silica gel column chromatography in an 19% yield (87.5 mg). HR-ESI-mass, *m/z* = 797.1418 (Calcd. [M]⁺ = 798.1447); ¹H NMR (CDCl₃, 600 MHz, ppm) δ 9.23 (s, 1H), 9.04–9.11 (m, 3H), 8.73 (s, 4H), 8.57 (s, 2H), 8.51 (s, 1H), 8.46 (d, *J* = 6 Hz, 1H), 7.17 (d, *J* = 6 Hz, 1H), 2.53 (s, 3H); UV-vis (CH₂Cl₂), λ_{max}/nm[ε × 10⁻⁵/(L·mol⁻¹·cm⁻¹): 413 (1.1793); ¹⁹F NMR (CDCl₃, ppm) δ 137.7, -152.5, -161.6.

2.6. Synthesis of **5**

H₃corrole **4** (79.8 mg, 0.1 mmol) and *cis*-[Pt(Me₂SO)₂Cl₂] **3** (42 mg, 0.1 mmol) was dissolved in 25 mL dry CH₂Cl₂ and stirred at 60 °C for 5 h under Ar atmosphere, after removal of organic solvent, the target compound **5** was obtained from recrystallization (CH₂Cl₂/EtOH) in an 88% yield (101.5 mg). HR-ESI-mass, *m/z* = 1063.0555 (Calcd. [M]⁺ = 1063.0532); ¹H NMR (CDCl₃, 600 MHz, ppm) δ 9.64 (s, 1H), 9.21 (d, *J* = 4.2 Hz, 2H), 8.88 (d, *J* = 4.2 Hz, 2H), 8.81 (d, *J* = 4.8 Hz, 2H), 8.66 (d, *J* = 3.6 Hz, 2H), 8.38 (d, *J* = 5.4 Hz, 1H), 7.92 (s, 1H), 7.43 (d, *J* = 18 Hz, 2H), 2.55 (s, 3H); UV-vis (CH₂Cl₂), λ_{max}/nm [ε × 10⁻⁵/(L·mol⁻¹·cm⁻¹): 417 (0.4081). ¹⁹F NMR (CDCl₃, ppm) δ

137.6, -151.7, -161.3.

3. Results and discussion

3.1. Synthesis and characterization

The free-base corrole compounds **4** were synthesized from a reaction of dipyrromethane **1** and the appropriate aryl-aldehyde (Scheme 1) according to the literature procedures.¹¹ The Pt complex **5** was synthesized from **4** and *cis*-[Pt(Me₂SO)₂Cl₂] **3**, were purified by recrystallization. High-resolution ESI-MS spectra revealed intense parent peaks at *m/z* = 797.1418 (Calcd. [M]⁺ = 798.1447) for **4** and *m/z* = 1063.0555 (Calcd. [M]⁺ = 1063.0532) for **5**, respectively. These results are providing direct evidence that the H₃corrole **4** and its Pt complex **5** were successfully prepared. The proton signals for the *meso*-substituted bipyridine and pyrrole rings in the ¹H NMR spectra of **4** (Fig. S5) lie beyond 7.16 ppm which is consistent with the presence of pentafluorophenyl rings at the *meso*-positions, and the peak at δ = 2.53 ppm for **4** could be assigned as the protons from methyl units. In the case of **5** (Fig. S7), due to the platinum(II) coordination, the protons from all pyridine rings were shifted to the lower field region, which lie beyond 7.41 ppm. ¹⁹F NMR spectra of **4** and **5** in CDCl₃ revealed similar peaks (Figs. S6 and S8) at δ = -137, -151 and -160 ppm.

3.2. Electronic structure

The UV-visible absorption and MCD spectra of H₃corrole **4** and its Pt(II)corrole **5** are measured in CH₂Cl₂ (Fig. 1). The electronic structure and optical spectroscopy of porphyrinoids can be readily understood by using Michl's perimeter model as a conceptual framework, through a consideration of the effect of structural perturbations on the molecular orbitals (MOs) of a C₁₆H₁₆²⁻ parent hydrocarbon perimeter corresponding to the inner ligand perimeter. When compared to the UV-visible absorption spectrum of the parent H₃-triphenylcorrole, less to no spectral changes were observed, due to the perturbation of bipyridine ring on the electronic structure is weak. The UV-vis absorption spectra of **4** reveals Soret band absorption at λ = 418 nm, while the Q-band absorptions were lie at λ = 568, 608, 642. When Pt atom was coordinated to bipyridine, complex **5** reveal slightly blue-shifted Soret band (λ = 414 nm) and Q-band absorption (λ = 560, 610, 640 nm). It should be pointed out here, Pt complex reveals an additional absorption band lie at λ = 352 nm assigned as the metal-to-ligand charge transfer from Pt atom to bipyridine ligand [28,29]. On the other hand, relatively clear Faraday B₀ terms are observed for each of these bands in the MCD spectrum of **4** and **5** as would normally be anticipated for metal porphyrinoids with four-fold symmetry due to there being orbitally non-degenerate excited states. The introduction of the *meso*-bipyridine and *meso*-[Pt^{II}(bipy)Cl₂]-substituent of the A₂B type corrole ligand has been considered to weakly interact with both HOMO and LUMO orbitals.

Moreover, **4** and **5** are also emitted with the moderate fluorescent properties for H₃corrole **4**, and significantly decreased result for **5** were observed, respectively (Fig. S9 and Table 1). This significant decrease of the fluorescent properties could be illustrated as the effective electron transfer between *meso*-[Pt^{II}(bipy)Cl₂]-substituent and the corrole aromatic core.

Cyclic voltammetry (CVs) and differential pulse voltammetry (DPVs) measurements revealed that Pt-corrole **5** has two reversible reduction curves at $E_{1/2}$ = -1.15 and -1.60 V (Fig. 2), respectively. These two reversible processes can be assigned to the 1st reduction of the Pt^{II} to Pt^I and the reduction of corrole ring itself, respectively. Moreover, a reversible curve is observed at $E_{1/2}$ = 1.12 V assigned as the corrole ring oxidation. When a comparison is made with the triarylcorroles using the same electrochemical characterization methods, no significant shifts of the reduction and oxidation steps are consistently observed except from the *meso*-[Pt^{II}(bipy)Cl₂]-substituent itself. The electrochemical behavior was also characterized by checking the effect of using various scan-speeds in non-aqueous media. The i_p^{Red} and i_p^{Ox} values, determined from CV measurements for **5** made at various scan-rates from 20 to 500 mV, provides an insight into the reversibility of the system on an experimental time-scale (Fig. S10, see ESI). The linear correlations confirm that all of the oxidation and reduction processes are diffusion controlled.

3.3. Electrocatalysis

Stability in acidic environments is an important consideration during the design of new HER catalysts. The stability of **5** was evaluated at acid media. The Pt-corrole **5** and H₂SO₄ (1:10 M ratio) were mixed in CH₃CN and were kept in the dark. Electronic absorption spectra were recorded at regular intervals for 4 h. Since negligible spectral changes are observed, it is safe to assume that **5** suitable for use as HER catalysts. It has been reported that Pt complexes could be efficiently used as molecular and/or single atom electrocatalysts for the electrochemically catalyzed hydrogen evolutions (HERs). Inspired by the above studies, we prepared a A₂B Corrole with a *meso*-[Pt^{II}(bipy)Cl₂]⁻ substituent to explore their electrocatalytic efficiency HERs. To evaluate the catalytic speed the conversion efficiency, linear sweep voltammetry (LSVs) of rGO supported **5** was tested in 0.5 M H₂SO₄ (Fig. 3). In the acid media, the Pt(II)corroles was exhibited as an excellent catalyst with overpotential E = -0.05 V (speed: 0.1 V/s; V vs RHE). More importantly, the Tafel slope was assigned as 59 mV/dec (speed: 0.1 V/s; V vs RHE) which was significantly lower than other transition metal-coordinated complexes (about 100–200 mV/dec), but only slightly higher than Pt/C nanocomposites (35 mV/dec). It should be mentioned here, that Pt^{II}(bipy)Cl₂ complex **6** (Figs. S11 and S12, see ESI) exhibits negative-shifted overpotential E = -0.25 V (speed: 0.1 V/s; V vs RHE) and increased Tafel slope 230 mV/dec (speed: 0.1 V/s; V vs RHE), that indicated the corrole ring plays and important role for charge transfer

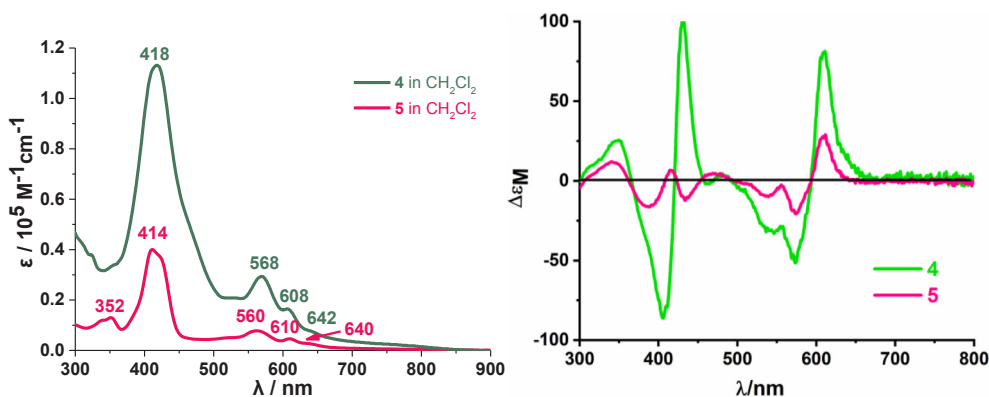


Fig. 1. UV-Vis absorption (left) and MCD (right) spectra of **4** and **5** in CH₂Cl₂.

Table 1
Fluorescent characterizations of 4 and 5.

cpd	λ_{ex} (nm)	λ_{em} (nm)	Φ_{F}	τ_{f} [ns]	$\Delta\mu$ (nm)	K_{r} [10^8 s^{-1}]	K_{nr} [10^8 s^{-1}]
4	410	652	5.04%	3.88	242	0.01299	0.2447
5	410	655	0.33%	0.94	245	0.00351	1.0603

Φ_{F} : Absolute quantum yield; $\Delta\mu$: Stokes's shift; K_{r} : Emission rate; K_{nr} : Non-emission rate.

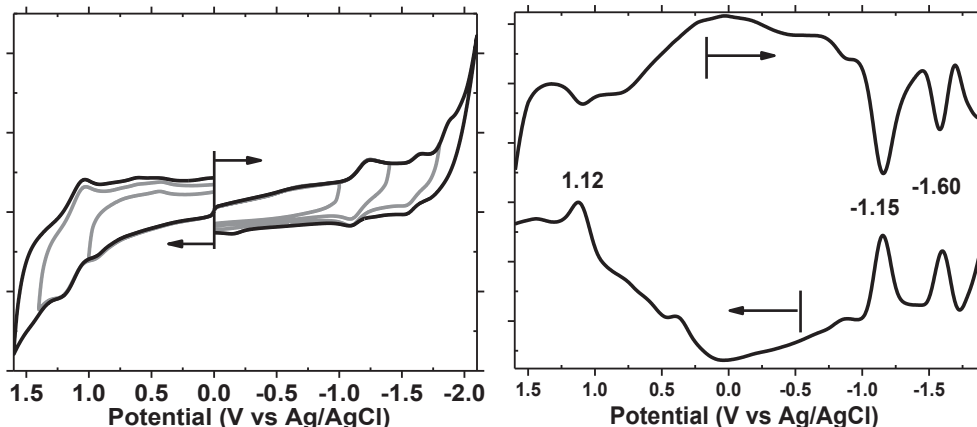


Fig. 2. CV and DPV measurements of Pt-corrole 5 in oDCB containing 0.1 M TBAP.

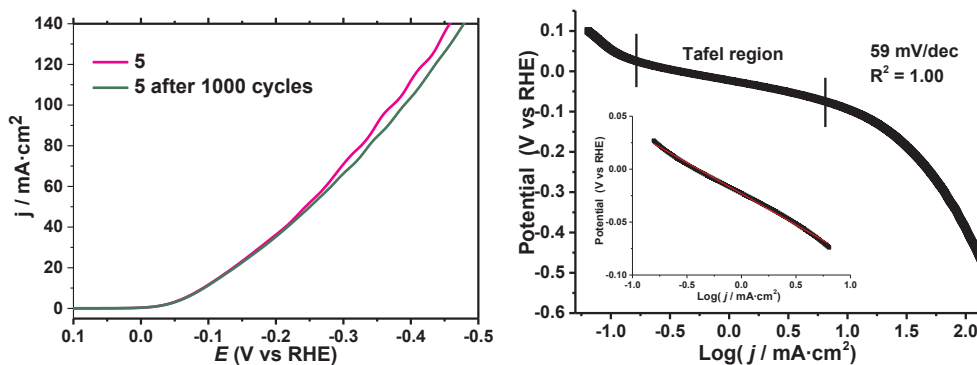


Fig. 3. LSV of rGO supported 5 and after 1000 cycles in 0.5 M H_2SO_4 (left) and the Tafel slope of rGO supported 5 in the same media (right).

between catalytic center and rGO supporters. On the other hand, the catalytic stability was also confirmed, and negligible changes on the LSV measurements were observed after 1000 cycles. All these results demonstrated that the Pt-corrole 5 exhibits efficient electrocatalytic hydrogen evolution behaviors, and the high conjugated corrole 18π aromatic ring were played essential media of the electron transfer process during the whole catalytic procedures.

4. Conclusion

In this manuscript, an A_2B Corrole with *meso*-bipyridine and *meso*- $[\text{Pt}^{\text{II}}(\text{bipy})\text{Cl}_2]$ -substituent were synthesized and isolated. Electronic structure was investigated by a detailed analysis of the UV–visible absorption and MCD spectra, cyclic and differential pulse voltammetry measurements, to identify the key trends in the redox and optical properties. Evidence for normally charge transfer between $\text{H}_3\text{corrole}$ macrocyclic ring and *meso*- $[\text{Pt}^{\text{II}}(\text{bipy})\text{Cl}_2]$ -substituent was observed. This study demonstrates that A_2B type corrole containing *meso*- $[\text{Pt}^{\text{II}}(\text{bipy})\text{Cl}_2]$ substituents are highly efficient catalysts for hydrogen evolutions with low overpotential (50 mV vs RHE for 5), low Tafel slope (59 mV/dec for 5) and robust catalytic behaviors. The efficient catalytic properties can be readily enhanced by charge transfer between bridging conjugated aromatic ring (corrole) and *meso*- $[\text{Pt}^{\text{II}}(\text{bipy})\text{Cl}_2]$ catalytic

center.

Acknowledgements

Financial support was provided by the National Scientific Foundation of China (No. 21701058 and 21606133), NSFC of Jiangsu province of China (no. BK20160499 and BK20160922) and the fund from the State Key Laboratory of Coordination Chemistry (SKLCC1817), the fund from Key Laboratory of Functional Inorganic Material Chemistry (Heilongjiang University) of Ministry of Education, the China post-doc foundation (No. 2018M642183), the Lanzhou High Talent Innovation and Entrepreneurship Project (No. 2018-RC-105) and the Jiangsu University (project 17JDG035).

Appendix A. Supplementary data

Supplementary data to this article can be found online at <https://doi.org/10.1016/j.ica.2019.119067>.

References

- [1] X. Liang, Y.J. Niu, Q.C. Zhang, J. Mack, X.Y. Yi, Z. Hlatshwayo, T. Nyokong, M.Z. Li, W.H. Zhu, Cu(III)triarylcorroles with asymmetric push-pull meso-substitutions: tunable molecular electrochemically catalyzed hydrogen evolution, Dalton Trans.

- (2017) 6912–6920.
- [2] H.L. Chen, G.Y. Lyu, Y.F. Yue, T.W. Wang, D.P. Li, H. Shi, J.N. Xing, J.Y. Shao, R. Zhang, J. Liu, Improving the photovoltaic performance by employing alkyl chains perpendicular to the p-conjugated plane of an organic dye in dye-sensitized solar cells, *J. Mater. Chem. C* 7 (2019) 7249–7258.
- [3] S. Garcia, M. Jose, S. Carlo, K. Mounika, S. Alexey, A. Kateryna, A. Plamen, I. Ioannis, Iron-streptomycin derived catalyst for efficient oxygen reduction reaction in ceramic microbial fuel cells operating with urine, *J. Power Sources* 425 (2019) 50–59.
- [4] G. Ajayakumar, M. Kobayashi, S. Masaoka, K. Sakai, Light-induced charge separation and photocatalytic hydrogen evolution from water using Ru(II)P(II)-based molecular devices: effects of introducing additional donor and/or acceptor sites, *Dalton Trans.* 40 (2011) 3955–3966.
- [5] Hironobu Ozawa, Masa-aki Haga, Ken Sakai, A photo-hydrogen-evolving molecular device driving visible-light-induced EDTA-reduction of water into molecular hydrogen, *J. Am. Chem. Soc.* 128 (2006) 4926–4927.
- [6] H. Ozawa, M. Kobayashi, B. Balan, S. Masaoka, K. Sakai, Photo-hydrogen-evolving molecular catalysts consisting of polypyridyl ruthenium(II) photosensitizers and platinum(II) catalysts: insights into the reaction mechanism, *Chem. Asian J.* 5 (2010) 1860–1869.
- [7] K.Y. Koo, H.J. Eom, U.H. Jung, W.L. Yoon, Ni nanosheet-coated monolith catalyst with high performance for hydrogen production via natural gas steam reforming, *Appl. Catal., A: General* 525 (2016) 103–109.
- [8] W.B. Jung, G.-T. Yun, Y. Kim, M. Kim, H.-T. Jung, Relationship between hydrogen evolution and wettability for multiscale hierarchical wrinkles, *ACS Appl. Mater. Inter.* 11 (7) (2019) 7546–7552.
- [9] M. Jiang, D.D. Zhu, J.J. Cai, H.Y. Zhang, X.B. Zhao, Electrocatalytic hydrogen evolution and oxygen reduction on polyoxotungstates/graphene nanocomposite multilayers, *J. Phys. Chem. C* 118 (26) (2014) 14371–14378.
- [10] A. Shi, H.H. Li, S. Yin, B. Liu, J.C. Zhang, Y.H. Wang, Photocatalytic NH_3 versus H_2 evolution over g-C₃N₄/CsxWO₃:O₂ and methanol tipping the scale, *Appl. Catal., B: Environ.* 218 (2017) 137–146.
- [11] K. Yamamoto, K. Kitamoto, K. Yamauchi, Ken Sakai, Pt(II)-Catalyzed photosynthesis for H_2 evolution cycling between singly and triply reduced species, *Chem. Commun.* 51 (2015) 14516–14519.
- [12] K. Kitamoto, K. Sakai, Pigment-acceptor-catalyst triads for photochemical hydrogen evolutions, *Angew. Chem. Int. Ed.* 53 (2014) 4618–4622.
- [13] Y.Q. Shi, W. Gao, H.Y. Lu, Y.P. Huang, L.Z. Zuo, W. Fan, T.X. Liu, Carbon-nanotube-incorporated graphene scroll-sheet conjoined aerogels for efficient hydrogen evolution reaction, *ACS Sustain. Chem. Eng.* 5 (8) (2017) 6994–7002.
- [14] M. Razavet, V. Artero, M.P. Fontecave, Electroreduction catalyzed by cobaloximes: functional models for hydrogenases, *Inorg. Chem.* 44 (13) (2005) 4786–4795.
- [15] A. Durairaj, T. Sakthivel, S. Thangavel, S. Vasanthkumar Ramanathan, Enhanced photocatalytic activity of transition metal ions doped g-C₃N₄ nanosheet activated by PMS for organic pollutant degradation, *ACS, Omega* 4 (4) (2019) 6476–6485.
- [16] W.H. Zhu, T.T. Huang, M.F. Qin, M.Z. Li, J. Mack, X. Liang, Tuning the synthetic cobalt(III)corroles electroreductive catalyzed lindane dehalogenation reactivity through meso-substituents, *J. Electroanal. Chem.* 774 (2016) 58–65.
- [17] W. Zhang, W.Z. Lai, R. Cao, Low overpotential water oxidation at neutral pH catalyzed by a copper(II) porphyrin, *Chem. Rev.* 117 (4) (2017) 3717–3797.
- [18] Y.J. Niu, M.Z. Li, Q.C. Zhang, W.H. Zhu, J. Mack, G. Fomo, T. Nyokong, X. Liang, Halogen substituted A2B type Co(III)triarylcorroles: synthesis, electronic structure and two step modulation of electrocatalyzed hydrogen evolution reactions, *Dyes Pigments* 142 (2017) 416–428.
- [19] M.Z. Li, Y.J. Niu, W.H. Zhu, J. Mack, G. Fomo, T. Nyokong, X. Liang, A₂B type copper(III)corroles containing zero-to-five fluorine atoms: synthesis, electronic structure and facile modulation of electrocatalyzed hydrogen evolution, *Dyes Pigments* 137 (2017) 523–531.
- [20] C.C.L. McCrory, S.H. Jung, J.C. Peters, T.F. Jaramillo, Benchmarking heterogeneous electrocatalysts for the oxygen evolution reaction, *J. Am. Chem. Soc.* 135 (2013) 16977–16987.
- [21] C.C.L. McCrory, S. Jung, I.M. Ferrer, S.M. Chatman, J.C. Peters, T.F. Jaramillo, Benchmarking hydrogen evolving reaction and oxygen evolving reaction electrocatalysts for solar water splitting devices, *J. Am. Chem. Soc.* 137 (2015) 4347–4357.
- [22] S.M. Tan, Z. Sofer, M. Pumera, Aromatic-exfoliated transition metal dichalcogenides: implications for inherent electrochemistry and hydrogen evolution, *Nanoscale* 7 (19) (2015) 8879–8883.
- [23] A.B. Alemayehu, H. Vazquez-Lima, C.M. Beavers, K.J. Gagnon, J. Bendix, A. Ghosh, Platinum corroles, *Chem. Commun.* 50 (2014) 11093–11096.
- [24] A.B. Abraham, L.J. McCormick, K.J. Gagnon, S.M. Borisov, A. Ghosh, Stable Platinum(IV) corroles: synthesis, molecular structure, and room-temperature near-IR phosphorescence, *ACS Omega* 3 (2018) 9360–9368.
- [25] K. Kitamoto, K. Sakai, Photochemical H_2 evolution from water catalyzed by dichloro(diphenylbipyridine)platinum(II) derivative tethered to multiple viologen acceptors, *Chem. Commun.* 47 (2011) 2227–2242.
- [26] M. Ogawa, G. Ajayakumar, S. Masaoka, H. Kraatz, K. Sakai, Platinum(II)-based hydrogen-evolving catalysts linked to multipendant viologen acceptors: experimental and DFT indications for bimolecular pathways, *Chem. Eur. J.* 17 (2011) 1148–1162.
- [27] S. Masaoka, Y. Mukawa, K. Sakai, Frontier orbital engineering of photo-hydrogen-evolving molecular devices: a clear relationship between the H_2 -evolving activity and the energy level of the LUMO, *Dalton Trans.* 39 (2010) 5868–5876.
- [28] B.A. Iglesias, J.F.B. Barata, P.M.R. Pereira, H. Girão, R. Fernandes, J.P.C. Tomé, M.G.P.M.S. Neves, A.S. Cavaleiro, New platinum(II)-bipyridyl corrole complexes: synthesis, characterization and binding studies with DNA and HSA, *J. Inorg. Biochem.* 153 (2015) 32–41.
- [29] D.F. Zigler, M.C. Elvington, J. Heinecke, K.J. Brewe, Luminescently tagged 2,2'-bipyridine complex of Fe(II): synthesis and photophysical studies of 4-[N-(2-Anthryl)carbamoyl]-4'-methyl-2,2'-bipyridine, *Inorg. Chem.* 45 (17) (2006) 6565–6567.